Int. J. Microgravity Sci. Appl., **36** (1) (2019) 360103
DOI: 10.15011//jasma.36.360103

|||| Original Paper ||||

X-ray Structure Analysis of Human Oxidized Nucleotide Hydrolase MTH1 using Crystals Obtained under Microgravity

Teruya NAKAMURA [1, 2], Keisuke HIRATA [2], Kana FUJIMIYA [3], Mami CHIRIFU [2], Takao ARIMORI [4], Taro TAMADA [5], Shinji IKEMIZU [2] and Yuriko YAMAGATA [2]

Abstract

Human MTH1 hydrolyzes oxidized nucleoside triphosphates with broad substrate specificity and draws attention as a potential anticancer target. Recently, we determined the high resolution crystal structures of MTH1 and suggested that MTH1 recognizes different substrates via an exchange of the protonation state at Asp119 and Asp120. In order to validate this mechanism, it is essential to observe hydrogen atoms by ultra-high resolution X-ray crystallography and/or neutron crystallography using large high quality crystals. Here we carried out the crystallization of MTH1 in complex with a substrate, 8-oxo-dGTP, under microgravity in the Japanese Experiment Module 'Kibo'. One of the crystals diffracted to 1.04-Å resolution, which is better than that we reported previously. We carried out bond length analysis of Asp119 and Asp120 using this updated data, which revealed the protonation state based on the bond lengths with higher accuracy and precision.

Keyword(s): Substrate specificity, Protonation, Aspartic acid
Received 16 October 2018, Accepted 8 January 2019, Published 31 January 2019.

1. Introduction

Reactive oxygen species generated during normal cellular metabolism oxidize not only DNA but also its precursor dNTP in the nucleotide pool. 8-Oxo-dGTP, one of the major oxidized nucleoside triphosphates, is a mutagenic substrate because it is incorporated opposite adenine as well as cytosine on the template strand by DNA polymerases [1)]. In *Escherichia coli*, MutT hydrolyzes 8-oxo-dGTP to 8-oxo-dGMP with quite high substrate specificity, and prevents transversion mutations caused by the misincorporation of 8-oxo-dGTP into DNA [1,2)]. The structural study on MutT revealed how MutT discriminates 8-oxoguanine nucleotides from normal guanine nucleotides with its high substrate specificity [3,4)]. In human, MutT homologue-1 (MTH1/NUDT1) is the counterpart of MutT, whose substrate specificity is different from that of MutT. MTH1 has broad substrate specificity for several oxidized nucleoside triphosphates including 8-oxo-dGTP and 2-oxo-dATP [5,6)], and is the main mammalian enzyme among other enzymes (NUDT5, MTH2/NUDT15, MTH3/NUDT18) responsible for sanitization of the nucleotide pool [7–10)]. In regard to the recognition and hydrolysis of oxidized nucleotides by these enzymes, crystal structures of NUDT5 in complex with the oxidized nucleotides and NMR analysis for its hydrolysis reaction provided the structural basis for the diverse recognition of substrates and a unique catalytic mechanism of NUDT5 [11)].

In 2014, human MTH1 was highlighted as a potential anticancer target because MTH1 highly expresses in cancer cells and avoids the misincorporation of oxidized nucleotides that result in DNA damage and cell death [12,13)]. Therefore, MTH1 blockade was suggested as a novel strategy for anticancer therapeutics. However, there are recent reports which have questioned this suggestion, and the efficacy of MTH1 inhibition in cancer cells is still under discussion [14,15)].

Previous mutational and NMR studies on MTH1 showed that Asp119, Trp117, Phe27 and Asn33 are important residues for substrate recognition and each residue has different contribution to the catalysis of 8-oxo-dGTP and 2-oxo-dATP [16,17)]. The crystal structure of MTH1-8-oxo-dGMP complex revealed that Asp119 and Asp120 form hydrogen bonds with 8-oxoguanine base (8-oxoG) [18)], and it was suggested that the protonation of Asp119 is required for the interaction with 8-oxoG [19)]. In addition, crystal structures of MTH1 in complex with inhibitors also showed that Asp119 and/or Asp120 make hydrogen bonds with all the inhibitors and are key residues for the design of more potent inhibitors [12–14,20–22)]. However, almost all the crystal structures were obtained at low pH and it was difficult to discuss the protonation state of Asp119 and Asp120 which is important information to understand the broad substrate specificity and the inhibitor-binding of MTH1.

1 Priority Organization for Innovation and Excellence, Kumamoto University, 5-1 Oe-honmachi, Chuo-ku, Kumamoto 862-0973, Japan.
2 Graduate School of Pharmaceutical Sciences, Kumamoto University, 5-1 Oe-honmachi, Chuo-ku, Kumamoto 862-0973, Japan.
3 School of Pharmacy, Kumamoto University, 5-1 Oe-honmachi, Chuo-ku, Kumamoto 862-0973, Japan.
4 Institute for Protein Research, Osaka University, 3-2 Yamadaoka, Suita, Osaka 565-0871, Japan.
5 Quantum Beam Science Research Directorate, National Institutes for Quantum and Radiological Science and Technology, 2-4 Shirakata, Tokai, Ibaraki 319-1106, Japan.
(E-mail: tnaka@gpo.kumamoto-u.ac.jp)

We previously reported that the MTH1(G2K) mutant with a homogeneous N-terminus produces high-quality crystals at neutral pH [23]. Recently, we have determined the crystal structures of MTH1(G2K) at neutral pH in complex with 8-oxo-dGTP and another good substrate 2-oxo-dATP, at 1.21- and 1.20-Å resolution, respectively [24]. These crystal structures and mutational analysis suggested that MTH1 recognizes the different substrates via an exchange of the protonation state at Asp119 and Asp120. In order to validate the mechanism, it is essential to observe hydrogen atoms by ultra-high resolution X-ray crystallography and/or neutron crystallography using large high quality crystals. Crystallization under microgravity has the advantage of being able to obtain large high quality crystals because microgravity condition eliminates convection effects near growing crystal surfaces [25]. Here, we carried out crystallization of MTH1 in complex with 8-oxo-dGTP under microgravity. Crystals were grown in the Japanese Experiment Module 'Kibo' of the International Space Station (ISS). X-ray diffraction data using the crystal were collected at 1.04-Å resolution which is better than that of the 8-oxo-dGTP complex we reported previously (1.21 Å). In addition, we refined the structure and carried out bond length analysis of Asp119 and Asp120 using the updated 1.04-Å resolution data and investigated the protonation state.

2. Protein Purification and Crystallization

For crystallization of MTH1 at neutral pH, MTH1(G2K/C87A/C104S) mutant was purified. The expression and purification were carried out as described previously [23,24], but a final purification step was newly added to improve the quality of crystallization sample. As the final step, MTH1 solution was applied to TSKgel SuperQ-5PW column (Tosoh) and eluted using a linear NaCl concentration gradient (buffer A, 20 mM Tris-HCl (pH 8.0); buffer B, 20 mM Tris-HCl (pH 8.0) and 0.5 M NaCl). The chromatogram showed two separated peak fractions containing MTH1. Native PAGE analysis of the two fractions showed that one contains homogeneous form but the other contains aggregated form. Then the purified homogeneous fractions were harvested and concentrated to 16.92 mg/mL of MTH1 for crystallization experiments.

For crystallization under microgravity, we applied the gel-tube method which is modified by JAXA based on the original counter-diffusion method [26–29]. In the experiments, we used glass capillaries (40 mm length, 0.5 mm diameter or 6 mm length, 1.9 mm diameter), protein solution (5.92 mg/mL MTH1, 6.3 mM 8-oxo-dGTP, 9.4 mM Tris-HCl (pH 8.0), 0.47 M sodium citrate, 47 mM NaCl, 0.05 M cacodylate (pH 6.5) or 0.05 M Tris-HCl (pH 7.0), 4.7% glycerol, 0.02% NaN_3), precipitant solution (1.37 mM 8-oxo-dGTP, 1 M sodium citrate, 0.2 M NaCl, 0.1 M cacodylate (pH 6.5) or 0.1 M Tris-HCl (pH 7.0), 10% glycerol) and pre-soaked solution (1 M sodium citrate, 0.2 M NaCl, 0.1 M cacodylate (pH 6.5) or 0.1 M Tris-HCl (pH 7.0), 10% glycerol). The crystallization device was assembled and micro-seeding was applied [30]. Crystals were grown under 293 K in the Protein Crystallization Research Facility on board the Japanese Experiment Module 'Kibo' of the ISS for 6 weeks. Crystals of the MTH1(G2K/C87A/C104S)-8-oxo-dGTP complex obtained using protein, precipitant and pre-soak solutions containing cacodylate (pH 6.5) are shown in **Fig. 1**.

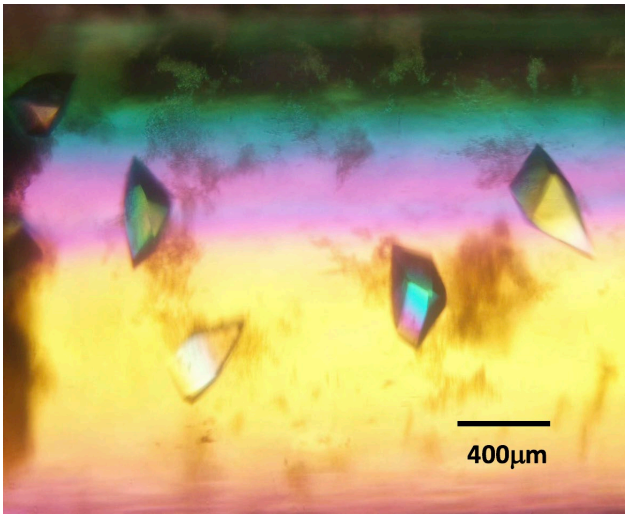

Fig. 1 Crystals of the MTH1(G2K/C87A/C104S)-8-oxo-dGTP complex grown under microgravity.

3. X-ray Data Collection and Structure Refinement

Crystals of the MTH1(G2K/C87A/C104S)-8-oxo-dGTP complex were transferred to a cryoprotectant solution supplemented with 20% glycerol and were frozen at 100 K by a nitrogen gas stream. X-ray diffraction experiments of the crystals were performed on beamlines at SPring-8 (Harima, Japan) and at Photon Factory (Tsukuba, Japan). The diffraction data used for the following structure determination were collected on BL44XU of SPring-8 using an X-ray wavelength of 0.9 Å with the MX-300 HE detector (Rayonix). Three data sets were collected at different positions in the same crystal, and were integrated, scaled and merged to 1.04-Å resolution using the program HKL2000 [31]. The X-ray data collection statistics are listed in **Table 1**. The resolution of this data is higher than that of the MTH1(G2K)-8-oxo-dGTP complex reported previously (PDB code: 5GHI, 1.21-Å resolution). Comparing the two data sets (1.04-Å vs 1.21-Å resolution), R_{merge} and $I/\sigma(I)$ in the resolution shell (1.23-1.20 Å) of the 1.04-Å resolution data set are 0.302 and 18.8, respectively, whereas those in the resolution shell (1.23-1.21 Å) of the 1.21-Å resolution data set are 0.433 and 2.8, respectively.

The structure was refined using the program PHENIX [32] with the structure of 5GHI as a starting model. The model was corrected using the program COOT [33]. Hydrogen atoms were automatically added to the model using PHENIX [32], but hydrogens at N atoms in the side chains of His and those in the nucleotides were removed. Asp and Glu are deprotonated forms. Anisotropic refinements except hydrogen atoms were applied. The R_{work}/R_{free} values (%) of the structure at 1.04-Å resolution were converged to 13.3/15.8. The refinement statistics are listed in **Table 2**. The atomic coordinates and the structure factors were deposited in the Protein Data Bank under accession code 6IJY. The bond length analysis to investigate the protonation state of Asp119 and Asp120 was carried out by unrestrained refinements using SHELXL [34] , and the refinement statistics are listed in **Table 3**.

Table 1 Data collection statistics

Wavelength (Å)	0.9
Space group	$P2_12_12_1$
Unit-cell lengths (Å)	a = 45.49 b = 48.10 c = 123.94
Resolution range (Å)	38.0-1.04 (1.06-1.04)
No. of observed reflections	1,657,713
No. of unique reflections	131,109
Completeness (%)	99.9 (100.0)
*R_{merge} (%)	10.9 (90.0)
$\langle I \rangle$ / $\langle \sigma(I) \rangle$	65.7 (4.8)

*R_{merge} = 100 x Σ_{hkl} Σ_i |I_i(hkl) - $\langle I(hkl) \rangle$| / Σ_{hkl} Σ_i I_i(hkl), where $\langle I(hkl) \rangle$ is the mean value of I(hkl).

Table 2 Refinement statistics using PHENIX

Resolution range (Å)	38.0-1.04
No. of reflections used	131,001
Completeness (%)	99.8
*R_{work} /R_{free} (%)	13.3/15.8
Ramachandran plot (%)	
Favored	99.7
Allowed	0.3
R.m.s.d. in bonds (Å)	0.008
R.m.s.d. in angles (deg.)	1.376

*R_{work} = 100 x $\Sigma||F_o| - |F_c||$ /$\Sigma|F_o|$. R_{free} was calculated from the test set (5% of the total data).

Table 3 Refinement statistics using SHELXL

Resolution range (Å)	38.0-1.04
No. of reflections used	130,992
Completeness (%)	100
*R_{work} /R_{free} (%)	13.0/15.4
Ramachandran plot (%)	
Favored	99.0
Allowed	1.0

*R_{work} = 100 x $\Sigma||F_o| - |F_c||$ /$\Sigma|F_o|$. R_{free} was calculated from the test set (5% of the total data).

4. Results and Discussion

There are two molecules (MolA and MolB) in the asymmetric unit of the crystal of MTH1(G2K/C87A/C104S)-8-oxo-dGTP. We use the structure of MolA for the following discussion because MolA shows clearer electron densities of 8-oxo-dGTP than MolB as is the case with the structure of 5GHI. The overall structure of MTH1(G2K/C87A/C104S)-8-oxo-dGTP is quite similar to that of 5GHI with root mean square deviation of 0.45 Å for the corresponding 156 Cα atoms although MTH1(G2K/C87A/C104S) has two additional mutation sites compared to MTH1(G2K). The binding mode of 8-oxo-dGTP is also identical to that in 5GHI. Briefly, the 8-oxoG base is recognized by a hydrogen bond with Asp119 (2.5 Å distance), two hydrogen bonds with Asp120 (2.8 Å and 2.9 Å distance, respectively) and two hydrogen bonds with Asn33 (2.8 Å and 3.0 Å distance, respectively) (**Fig. 2**).

The bond length analysis using high resolution X-ray structures has been performed to determine the protonation

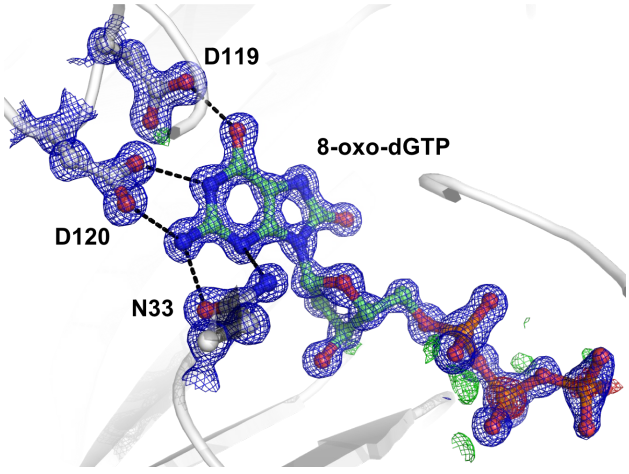

Fig. 2 Binding mode of 8-oxo-dGTP. 8-Oxo-dGTP, Asp119, Asp120 and Asn33 are shown in ball and stick representation. $2F_o-F_c$ map (blue) and F_o-F_c map (positive, green; negative, red) are contoured at 2.0σ and 3.5σ, respectively. Molecular graphics were drawn using PyMOL [35].

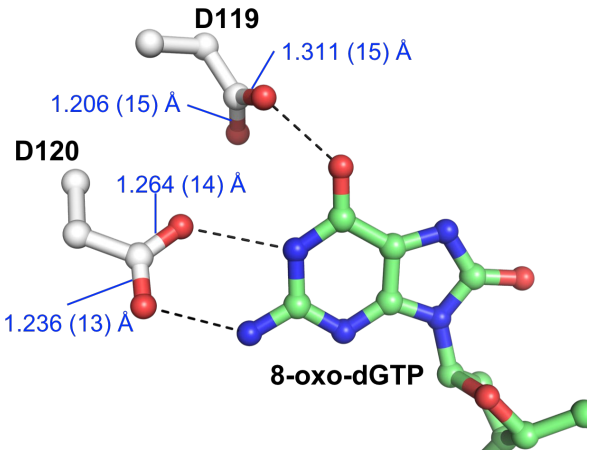

Fig. 3 Bond lengths with estimated standard deviations of Asp119 and Asp120 after the unrestrained refinements using SHELXL.

states of ionizable residues such as Asp and Glu [36,37]. In the carboxylic group (protonated state), the expected bond lengths of the C=O and C-OH bonds are 1.21 and 1.31 Å, respectively. While, in the delocalized carboxylate group (deprotonated state), the C-Oδ1 and C-Oδ2 bonds have similar bond lengths, 1.26 Å [36]. Previous bond lengths analysis of Asp119 and Asp120 by the unrestrained refinements with 1.21-Å resolution data showed that C-Oδ1 and C-Oδ2 of Asp119 are 1.313 (32) and 1.200 (31) Å, respectively, whereas those of Asp120 are 1.254 (27) and 1.198 (26) Å, respectively [24]. Values in parentheses show the estimated standard deviations of bond lengths calculated by SHELXL. There is a significant difference in the two bond lengths of Asp 119 at 4σ level, whereas no significant difference was found in the two bond lengths of Asp120 when considered with the σ values, indicating that Asp119 is protonated and Asp120 is deprotonated to make hydrogen bonds with 8-oxo-dGTP. The updated 1.04 Å structure after the unrestrained refinements showed bond lengths closer to the ideal ones [36] and smaller associated standard deviations; that is, C-Oδ1 and C-Oδ2 of Asp119 are 1.311 (15) and 1.206 (15) Å, respectively, whereas those of Asp120 are 1.264 (14) and 1.236 (13) Å, respectively (**Fig. 3**). These results also showed that protonated Asp119 and deprotonated Asp120 are required for the recognition of 8-oxo-dGTP.

Here, we obtained crystals of the MTH1-8-oxo-dGTP complex under microgravity and determined the 1.04-Å resolution structure. In order to obtain large high quality crystals for ultra-high resolution X-ray crystallography and/or neutron crystallography, further refinements of the crystallization conditions are in progress.

Acknowledgement

This study is contributed by a part of "High-Quality Protein Crystal Growth Experiment on KIBO" promoted by JAXA (Japan Aerospace Exploration Agency). Russian Space craft "Progress" or/and "Soyuz" provided by Russian Federal Space Agency were used for space transportation. A part of space crystallization technology had been developed by European Space Agency and University of Granada. We thank H. Tanaka, S. Takahashi, B. Yan, N. Furubayashi and K. Inaka for assistance with protein purification and crystal preparation using new seeding method for capillaries. We also thank the beamline staff at SPring-8 and at Photon Factory for X-ray experiments, and M. A. Suico for critical reading of the manuscript. This study was supported by Grants-in-Aid for Scientific Research (T.N.) and Photon and Quantum Basic Research Coordinated Development Program (Y.Y.) from the Ministry of Education, Culture, Sports, Science and Technology of Japan and by The Nakajima Foundation (T.N.).

References

1) H. Maki and M. Sekiguchi: Nature, **355** (1992) 273.
2) R. Ito, H. Hayakawa, M. Sekiguchi and T. Ishibashi: Biochemistry, **44** (2005) 6670.
3) T. Nakamura, S. Meshitsuka, S. Kitagawa, N. Abe, J. Yamada, T. Ishino, H. Nakano, T. Tsuzuki, T. Doi, Y. Kobayashi, S. Fujii, M. Sekiguchi and Y. Yamagata: J. Biol. Chem., **285** (2010) 444.
4) T. Nakamura, T. Doi, M. Sekiguchi and Y. Yamagata: Acta Crystallogr. Sect. D Biol. Crystallogr.,**60** (2004) 1641.
5) J.Y. Mo, H. Maki and M. Sekiguchi: Proc. Natl. Acad. Sci. U. S. A., **89** (1992) 11021.
6) K. Fujikawa, H. Kamiya, H. Yakushiji, Y. Fujii, Y. Nakabeppu and H. Kasai: J. Biol. Chem., **274** (1999) 18201.
7) T. Ishibashi, H. Hayakawa and M. Sekiguchi: EMBO Rep., **4** (2003) 479.
8) T. Ishibashi, H. Hayakawa, R. Ito, M. Miyazawa, Y. Yamagata and M. Sekiguchi: Nucleic Acids Res., **33** (2005) 3779.
9) Y. Takagi, D. Setoyama, R. Ito, H. Kamiya, Y. Yamagata and M. Sekiguchi: J. Biol. Chem., **287** (2012) 21541.
10) M. Carter, A.-S. Jemth, A. Hagenkort, B.D.G. Page, R. Gustafsson, J.J. Griese, H. Gad, N.C.K. Valerie, M. Desroses, J. Boström, U. Warpman Berglund, T. Helleday and P. Stenmark: Nat. Commun., **6** (2015) 7871.
11) T. Arimori, H. Tamaoki, T. Nakamura, H. Kamiya, S. Ikemizu, Y. Takagi, T. Ishibashi, H. Harashima, M. Sekiguchi and Y. Yamagata: Nucleic Acids Res., **39** (2011) 8972.
12) H. Gad, T. Koolmeister, A.-S. Jemth, S. Eshtad, S.A. Jacques, C.E. Ström, L.M. Svensson, N. Schultz, T. Lundbäck, B.O. Einarsdottir, A. Saleh, C. Göktürk, P. Baranczewski, R. Svensson, R.P.-A. Berntsson, R. Gustafsson, K. Strömberg, K. Sanjiv, M.-C. Jacques-Cordonnier, M. Desroses, A.-L. Gustavsson, R. Olofsson, F. Johansson, E.J. Homan, O. Loseva, L. Bräutigam, L. Johansson, A. Höglund, A. Hagenkort, T. Pham, M. Altun, F.Z. Gaugaz, S. Vikingsson, B. Evers, M. Henriksson, K.S.A. Vallin, O.A. Wallner, L.G.J. Hammarström, E. Wiita, I. Almlöf, C. Kalderén, H. Axelsson, T. Djureinovic, J.C. Puigvert, M. Häggblad, F. Jeppsson, U. Martens, C. Lundin, B. Lundgren, I. Granelli, A.J. Jensen, P. Artursson, J.A. Nilsson, P. Stenmark, M. Scobie, U.W. Berglund and T. Helleday: Nature, **508** (2014) 215.
13) K.V.M. Huber, E. Salah, B. Radic, M. Gridling, J.M. Elkins, A. Stukalov, A.-S. Jemth, C. Göktürk, K. Sanjiv, K. Strömberg, T. Pham, U.W. Berglund, J. Colinge, K.L. Bennett, J.I. Loizou, T. Helleday, S. Knapp and G. Superti-Furga: Nature, **508** (2014) 222.

14) J.G. Kettle, H. Alwan, M. Bista, J. Breed, N.L. Davies, K. Eckersley, S. Fillery, K.M. Foote, L. Goodwin, D.R. Jones, H. Käck, A. Lau, J.W.M. Nissink, J. Read, J.S. Scott, B. Taylor, G. Walker, L. Wissler and M. Wylot: J. Med. Chem., **59** (2016) 2346.
15) A. Petrocchi, E. Leo, N.J. Reyna, M.M. Hamilton, X. Shi, C.A. Parker, F. Mseeh, J.P. Bardenhagen, P. Leonard, J.B. Cross, S. Huang, Y. Jiang, M. Cardozo, G. Draetta, J.R. Marszalek, C. Toniatti, P. Jones and R.T. Lewis: Bioorg. Med. Chem. Lett., **26** (2016) 1503.
16) Y. Sakai, M. Furuichi, M. Takahashi, M. Mishima, S. Iwai, M. Shirakawa and Y. Nakabeppu: J. Biol. Chem., **277** (2002) 8579.
17) M. Mishima, Y. Sakai, N. Itoh, H. Kamiya, M. Furuichi, M. Takahashi, Y. Yamagata, S. Iwai, Y. Nakabeppu and M. Shirakawa: J. Biol. Chem., **279** (2004) 33806.
18) L.M. Svensson, A.-S. Jemth, M. Desroses, O. Loseva, T. Helleday, M. Högbom and P. Stenmark: FEBS Lett., **585** (2011) 2617.
19) T. Nakamura, Y. Kitaguchi, M. Miyazawa, H. Kamiya, S. Toma, S. Ikemizu, M. Shirakawa, Y. Nakabeppu and Y. Yamagata: Acta Crystallogr. Sect. F Struct. Biol. Cryst. Commun., **62** (2006) 1283.
20) J.W.M. Nissink, M. Bista, J. Breed, N. Carter, K. Embrey, J. Read and J.J. Winter-Holt: PLoS ONE, **11** (2016) e0151154.
21) A. Rudling, R. Gustafsson, I. Almlöf, E. Homan, M. Scobie, U. Warpman Berglund, T. Helleday, P. Stenmark and J. Carlsson: J. Med. Chem., **60** (2017) 8160.
22) F. Rahm, J. Viklund, L. Trésaugues, M. Ellermann, A. Giese, U. Ericsson, R. Forsblom, T. Ginman, J. Günther, K. Hallberg, J. Lindström, L.B. Persson, C. Silvander, A. Talagas, L. Díaz-Sáez, O. Fedorov, K.V.M. Huber, I. Panagakou, P. Siejka, M. Gorjánácz, M. Bauser and M. Andersson: J. Med. Chem., **61** (2018) 2533.
23) Y. Koga, M. Inazato, T. Nakamura, C. Hashikawa, M. Chirifu, A. Michi, T. Yamashita, S. Toma, A. Kuniyasu, S. Ikemizu, Y. Nakabeppu and Y. Yamagata: Acta Crystallogr. Sect. F Struct. Biol. Cryst. Commun., **69** (2013) 45.
24) S. Waz, T. Nakamura, K. Hirata, Y. Koga-Ogawa, M. Chirifu, T. Arimori, T. Tamada, S. Ikemizu, Y. Nakabeppu and Y. Yamagata: J. Biol. Chem., **292** (2017) 2785.
25) W. Littke and C. John: J. Cryst. Growth, **76** (1986) 663.
26) J.M. García-Ruiz and A. Morena: Acta Crystallogr. Sect. D Biol. Crystallogr., **50** (1994) 484.
27) L.A. González-Ramírez, J. Carrera, J.A. Gavira, E. Melero-García and J.M. García-Ruiz: Cryst. Growth Des., **8** (2008) 4324.
28) F. Otálora, J.A. Gavira, J.D. Ng and J.M. García-Ruiz: Prog. Biophys. Mol. Biol., **101** (2009) 26.
29) H. Tanaka, K. Inaka, S. Sugiyama, S. Takahashi, S. Sano, M. Sato and S. Yoshitomi: J. Synchrotron Radiat., **11** (2004) 45.
30) S. Takahashi, M. Koga, B. Yan, N. Furubayashi, M. Kamo, K. Inaka and H. Tanaka: Int. J. Microgravity Sci. Appl., **1** (2019) 360107.
31) Z. Otwinowski and W. Minor: Methods Enzymol., **276** (1997) 307.
32) P.D. Adams, P. V. Afonine, G. Bunkóczi, V.B. Chen, I.W. Davis, N. Echols, J.J. Headd, L.-W. Hung, G.J. Kapral, R.W. Grosse-Kunstleve, A.J. McCoy, N.W. Moriarty, R. Oeffner, R.J. Read, D.C. Richardson, J.S. Richardson, T.C. Terwilliger and P.H. Zwart: Acta Crystallogr. Sect. D Biol. Crystallogr., **66** (2010) 213.
33) P. Emley and K. Cowtan: Acta Crystallogr. Sect. D Biol. Crystallogr., **60** (2004) 2126.
34) G.M. Sheldrick: Acta Crystallogr. Sect. C Struct. Chem., **71** (2015) 3.
35) The PyMOL Molecular Graphics System, Version 2.0 Schrödinger, LLC.
36) H.U. Ahmed, M.P. Blakeley, M. Cianci, D.W.J. Cruickshank, J.A. Hubbard and J.R. Helliwell: Acta Crystallogr. Sect. D Biol. Crystallogr., **63** (2007) 906.
37) S.J. Fisher, M.P. Blakeley, M. Cianci, S. McSweeney and J.R. Helliwell: Acta Crystallogr. Sect. D Biol. Crystallogr., **68** (2012) 800.